Corrosion of Nuclear Fuel Inside a Failed Nuclear Waste Container

D.W. Shoesmith and J.J. Noël
Department of Chemistry
University of Western Ontario
London, ON Canada N6A 5B7

F. Garisto
Ontario Power Generation
700 University Avenue
Toronto, ON Canada M5G 1X6

ABSTRACT

A mixed-potential model to predict the corrosion behaviour of nuclear fuel inside a failed carbon steel-lined copper waste container in a deep geologic repository is briefly described. A number of experiments underway to improve the mechanistic form of the model and to provide the necessary input data are discussed. A primary emphasis is placed on the consequences of the accumulation of corrosion product deposits on the fuel surface on the development of aggressive local chemistries, the cathodic reduction of H_2O_2 and the potential for scavenging of H_2O_2 by the products of carbon steel corrosion (in particular H_2).

INTRODUCTION

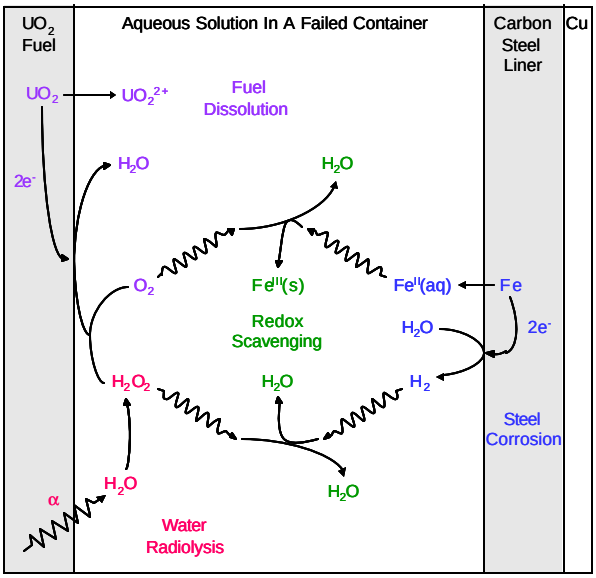

Figure 1: Corrosion scenario within a failed Cu waste container.

A primary requirement in the development of performance assessment models for the permanent disposal of nuclear fuel is a model to predict the corrosion rate of nuclear fuel inside a failed waste container. The prospects for long term containment using a copper waste container are very good [1]. Nevertheless, it is judicious to analyze the potential consequences of failure while the production of radiolytic oxidants within a groundwater-flooded container still exists. Since gamma (γ) and beta (β) radiation fields become insignificant for times $>10^3$ years, it seems reasonable to consider only the potential effects of alpha (α) radiation [2]. Recently [3], we have described a mixed potential model to predict the corrosion behaviour of fuel by α-radiolytically decomposed water within a failed copper nuclear waste container internally supported with a carbon steel liner or carbon steel insert. Figure 1

summarizes the key reactions included in this model. A fuller description of the reactions included as well as the details of its mathematical formulation, are described elsewhere [3].

The model consists of two corrosion fronts, one on the fuel surface and a second on the steel surface, interconnected by diffusion processes in the groundwater. Depending on the time of container failure and, hence, the alpha dose rate available at the fuel surface, the redox gradient between these two surfaces (expressed as a difference in corrosion potentials) could be between −600 and −900mV. Thus, the diffusive mixing of corrosion products will lead to homogeneous redox reactions which could scavenge radiolytic oxidants thereby reducing the fuel corrosion potential and suppressing fuel corrosion and radionuclide release. Sensitivity calculations using this model indicate that key issues in determining fuel corrosion rates are the kinetics of fuel dissolution and how it is influenced by the presence of corrosion product deposits, the kinetics of H_2O_2 reduction to support anodic fuel dissolution, and the possibility of scavenging H_2O_2 by reaction with the products of carbon steel corrosion.

Influence of Redox Conditions on Fuel Corrosion

The expected behaviour of a UO_2 surface as a function of surface redox condition (expressed as a corrosion potential) is summarized in Figure 2. The chemical composition of the fuel surface and the ranges of different chemical/electrochemical behaviour have been determined using a range of electrochemical and surface analytical techniques [2,4]. The onset of observable oxidation occurs around -450 mV (vs SCE), the lowest potential for which an increase in U(V) content of the fuel surface can be observed by x-ray photoelectron spectroscopy [4]. Over the potential range –450 mV to ~ 0 mV, the ratio U(V)/U(IV) in the fuel surface increases due to a change in surface composition and/or an increase in thickness of a thin surface layer (2 to 8 nm). For potentials > 0 mV, the formation of U(VI) species (as a $UO_3 \cdot xH_2O$ deposit) occurs on the fuel surface [4]. Previous electrochemical studies detected dissolution at potentials as low as ~ -300 mV [5]. This reflects a detection limit not a real potential threshold and it seems judicious to assume that dissolution becomes feasible as soon as oxidation of the fuel surface commences. The bar marked A in Figure 2 indicates the range of fuel corrosion potentials predicted by the MPM [3] from first contact with groundwater, neglecting β/γ radiation. A comparison of this prediction to the potential thresholds

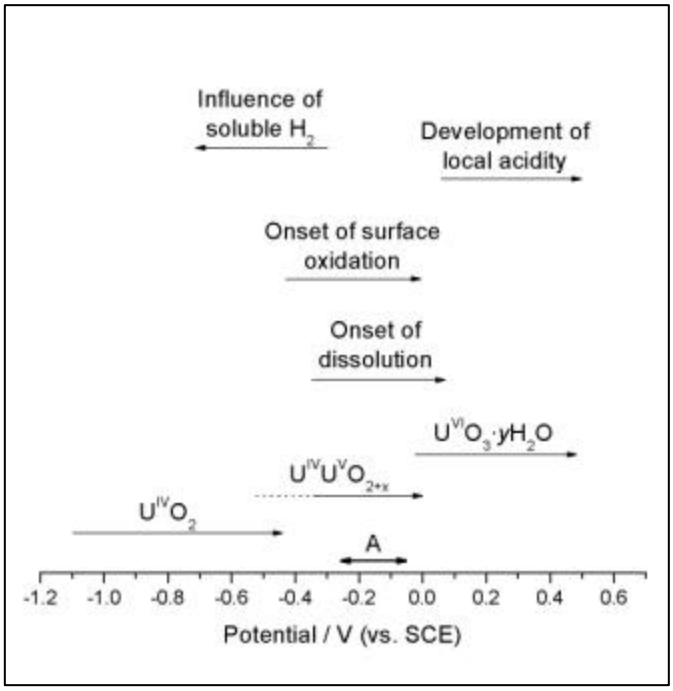

Figure 2: Expected behavior of a UO_2 surface as a function of redox condition (expressed as a corrosion potential).

indicates that the surface redox condition of the fuel will always be in the range where corrosion is feasible.

The Influence of Corrosion Product Deposits

The presence of a corrosion product deposit would be expected to suppress dissolution by blocking surface sites to an extent determined by its porosity. The influence of porosity is incorporated into the MPM but is difficult to quantify experimentally. For E >50 mV rapid fuel dissolution and uranyl ion hydrolysis produces acidity within the pores of the deposit [4,6], as illustrated schematically in Figure 3. While primarily within pores in the deposit, acidity will also be trapped within pores and defects in the fuel surface itself. In the absence of acidification, these pores would be expected to seal by precipitation since the dissolving fuel surface will be the site of highest U(VI) concentration. However, the development of acidity introduces a pH gradient within the pores and, hence a chemical driving force (based on the pH dependence of solubility) which would maintain porosity and sustain film growth, Figure 4.

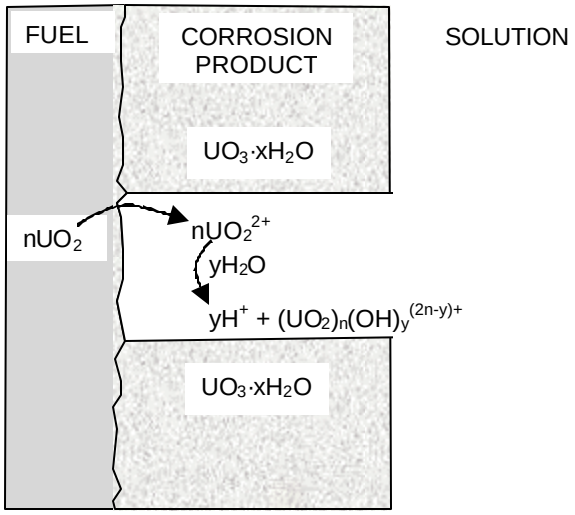

Figure 3: Schematic illustrating the formation of acidity within a pore in a corrosion product deposit.

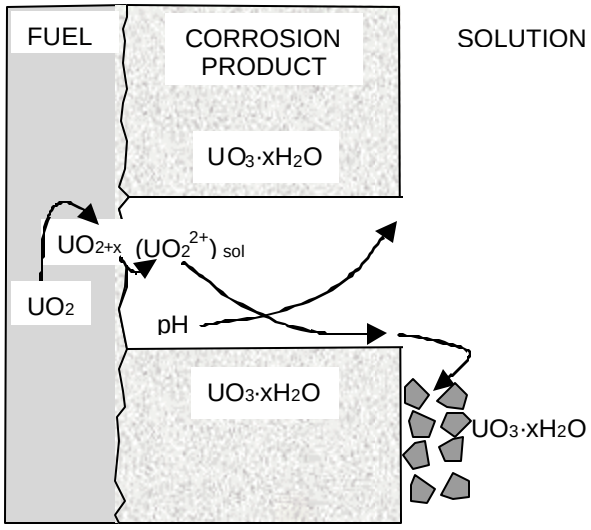

Figure 4: Schematic illustrating the possible influence of a pH gradient on the maintenance of open porosity in corrosion product deposits.

The presence of a deposit could not only partially block the fuel corrosion process but, if eventually thick enough, could control the local redox conditions at the fuel surface. This could occur by a number of processes as illustrated schematically in Figure 5: (i) the redistribution of long-lived alpha emitters by dissolution and incorporation in the corrosion product deposit could lead to a three dimensional radiation field [7]; (ii) the accumulation of an insoluble residue of alpha emitters on the fuel surface could enhance radiolysis within pores [8]; and (iii) the confinement of radiolytic oxidants within the pores and the limited access of potential redox scavengers could increase the local redox potential at the fuel surfaces.

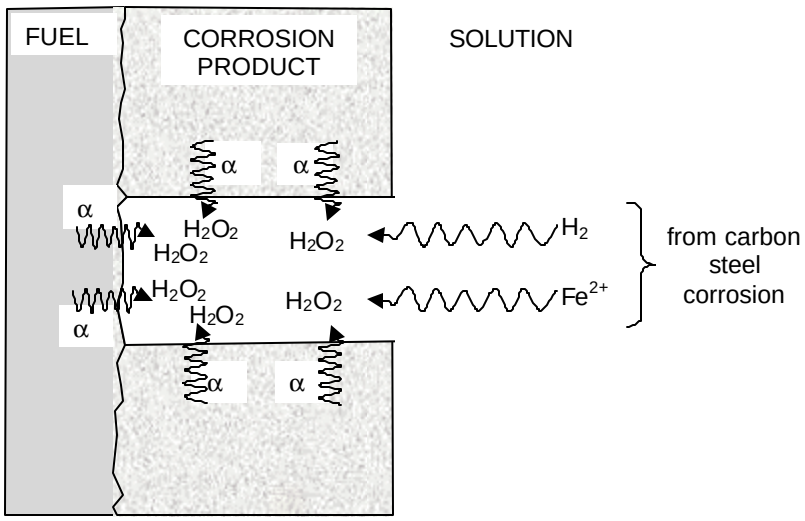

Figure 5: Schematic illustrating the processes that could control redox conditions within pores in a corrosion product deposit.

Presently, we are studying the influence of groundwater species on the chemistry within such pores. The switch from a Na^+- to a Ca^{2+}-dominated groundwater significantly suppresses the development of local acidity without incorporation of Ca^{2+} into the deposit, at least in short term experiments [9]. This suppression can be attributed to an electrostatic effect and is consistent with the observed influence of Ca^{2+} on rates measured in longer-term flow-through experiments [10,11]. At pH~ 9.5 (at which our electrochemical tests were conducted), the $UO_2/UO_{2+x}/UO_3 \cdot xH_2O$ surface will be negatively charged and the availability of protons low. The electrostatic interaction of the strongly polarizing Ca^{2+}-ion with the fuel surface appears to inhibit the anion transfer process across the oxide/solution interface essential to overall dissolution.

Preliminary electrochemical and XPS studies on silicate, another groundwater constituent, indicate that, unlike Ca^{2+}, this ion is incorporated into corrosion product deposits, presumably to form a lower solubility uranyl-containing solid [12]). Suppression of acidity development and a decrease in UO_2^{2+} solubility would both be expected to close down porosity and slow fuel corrosion. Since it has proven difficult to investigate the porosity of corrosion product deposits on a laboratory time frame, we are attempting to model the relationship between pore dimension, fuel corrosion rate and acidity development.

Kinetics of Hydrogen Peroxide Reduction/Decomposition

Sensitivity calculations using the MPM [13] show that the rate constant for the primary cathodic reaction, H_2O_2 reduction, has a very large effect on the effective G-value (a measure of the utilization of radiolytic oxidants to cause fuel corrosion). For this reaction to occur, the fuel surface must be conducting; i.e. oxidized to a mixed U(IV)/U(V) state. The presence of insulating U(VI) surface species (E > 50 mV, Figure 2) inhibits both H_2O_2 reduction and its decomposition to O_2 and H_2O. Decomposition of H_2O_2 becomes regulated to either the release rate of U(VI) species from the surface, or the rate at which O_2 (from H_2O_2 decomposition) is consumed by fuel corrosion.

The E_{CORR} range predicted by the MPM (A in Figure 2) indicates that H_2O_2 reduction should always be possible on the fuel surface but the potential will be too low to support even slow

peroxide decomposition. Electrochemical studies show that H_2O_2 reduction proceeds by the creation of a surface-conducting U(V) site,

$$2U(IV) + H_2O_2 \rightarrow 2U(V) + 2OH^-$$

followed by the electrochemical regeneration of the reduced surface site [14],

$$2U(V) + 2e^- \rightarrow 2U(IV)$$

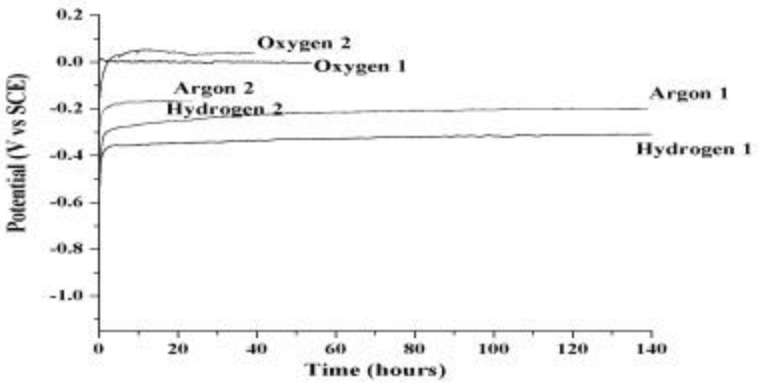

Figure 6: Corrosion potentials measured on SIMFUEL electrodes containing (1), and not containing (2), ε-particles in 0.1 mol/L KCl (pH ~ 9.5) purged with air,

As described elsewhere in these proceedings, carbonate has an influence on H_2O_2 reduction as well as its clearly demonstrated effect on the anodic dissolution kinetics [2,15]. Peroxide reduction is catalyzed close to the corrosion potential by a U – CO_3 - H_2O_2 surface complex. Since this species is formed at oxidizing potentials and can support electron transfer to H_2O_2 we assume, but have not proven, that it involves a U(V) carbonate complex able to coordinate H_2O_2 and act as a donor-acceptor site [2]. This effect disappears for carbonate concentrations $\leq 10^{-3}$ mol/L and should not exert a major influence on fuel corrosion in low carbonate-containing groundwaters. Because of these mechanistic complications, the measurement of a more certain rate constant for the cathodic reduction of peroxide for use in the MPM has proven elusive. Presently, we are studying peroxide reduction as a function of pH since its reduction within pores in a corrosion product deposit may occur under more acidic conditions, and the production of OH^- would neutralize, at least partially, the development of acidity within such pores.

Scavenging of Radiolytic Oxidants

Both Fe(II) and H_2 from steel corrosion are potential scavengers for H_2O_2, but presently only the reaction of Fe^{2+} with H_2O_2 is included in the MPM. Sensitivity studies [13] suggest this reaction will exert only a minor effect on the overall corrosion rate because of the low solubility of Fe (II) at anticipated groundwater pH values. However, in sealed repositories substantial hydrogen pressures, leading to dissolved H_2 concentrations in the 10^{-2} to 10^{-1} mol/L range, are anticipated, and H_2 has been shown to have a very strong influence on radionuclide leaching and fuel corrosion rates [16,17]. Also, H_2 has been shown to reduce the extent of fuel oxidation in the presence of both alpha and gamma radiation [18,19]. This influence of gamma radiation fields is not surprising since standard radiolysis models show that moderate H_2 concentrations (~10^{-5} mol/L) suppress H_2O_2 production via radical reactions [20]. Using external gamma sources it was shown [19] that H_2 pressures of 5 MPa suppressed the fuel corrosion potential to values (~ −700 mV vs SCE) well below that for the onset of UO_2 oxidation, Figure 2, suggesting a direct reducing effect on the UO_2 surface. Since molecular H_2 is generally chemically inert for T $\leq 100^oC$, these results suggest the reaction of radiolytically-produced $H^\bullet$ with the fuel surface.

Recently, we have begun studying the possibility that the fuel surface itself will be catalytic for the production of $H^{\bullet}$ radicals even in the absence of radiation fields. Figure 6 shows corrosion potentials measured on a 1.5 at.% SIMFUEL electrode in 0.1 mol/L KCl (pH~9.5) purged with either air, Ar or H_2 at 60°C. This material is an unirradiated analogue of used nuclear fuel, produced by doping a UO_2 matrix with a series of stable elements to simulate the chemical effects of a 1.5 At% in-reactor burn-up. As expected, the corrosion potential differs for aerated and anoxic (Ar-purged) conditions, but the even lower potential observed for H_2 – purged conditions indicates the establishment of reducing as opposed to simply anoxic conditions. Similar experiments on a SIMFUEL electrode which does not contain ε-particles, Figure 6, show the corrosion potentials in Ar-purged (anoxic) and H_2-purged solutions are identical, supporting the argument that the H_2/H^+ reaction is catalyzed on ε-particles, which act like galvanically-coupled cathodes within the fuel matrix, leading to the suppression of surface redox conditions and the inhibition of fuel oxidation. A more extensive series of electrochemical and surface analytical experiments is underway to confirm this hypothesis.

ACKNOWLEDGEMENTS

This research was funded under the Industrial Research Chair agreement between the Canadian Natural Sciences and Engineering Research Council (NSERC) and Ontario Power Generation, Toronto, CA. We are grateful to M.Broczkowski for the data in Figure 6.

REFERENCES

1. F. King and M. Kolar. Ontario Power Generation Report No: 06819-REP-01200-10041-1200-R00 (2000).
2. D.W. Shoesmith, *J. Nucl. Mater*. **282**, 1 (2000).
3. D.W. Shoesmith, M. Kolar and F. King, *Corrosion* **59**, 802 (2003)
4. B.G. Santos, H.W. Nesbitt, J.J. Noel and D.W. Shoesmith, *Electrochimica Acta*, **49**, 1863 (2004).
5. J.D. Rudnicki, R. Russo and D.W. Shoesmith, *J. Electroanal. Chem*. **372**, 3 (1994).
6. S. Sunder, L.K. Strandlund and D.W. Shoesmith, *Electrochimica Acta,* **43**, 2359 (1998).
7. C.W. Kim, D.J. Wronkiewicz and E.C. Buck, *Mat. Res. Soc. Symp. Proc*. **608**, 47 (2000)
8. E.C. Buck, P.A. Finn and J.K. Bates, *Micron*, **35**, 235 (2004)
9. B.G. Santos, J.J. Noel and D.W. Shoesmith, unpublished data.
10. C.N. Wilson and W.J. Gray, *Mat. Res. Soc. Symp. Proc*. **176**, 489 (1990).
11. J.C. Tait and J.L.M. Luht, Ontario Hydro Report No: 06819-REP-01200-0006-1200-R00 (1997).
12. J.L.M. Luht, M.Sc. Thesis, University of Manitoba, Winnipeg, Canada (1998)
13. F. King and M. Kolar, Ontario Power Generation Report No: 06819-REP-01300-10044-12-R00 (2002).
14. J.G. Goldik, H.W. Nesbitt, J.J. Noel and D.W. Shoesmith, *Electrochimica Acta*, **49**, 1699 (2004).

15. J. dePablo, I. Casas, J. Gimenez, V. Marti and M.E. Torrero, *J. Nucl Mater*. **232**, 138 (1996).
16. K. Spahiu, L. Werme and U-B Eklind, *Radiochim. Acta*, **88**, 507 (2000).
17. S. Rollin, K. Spahiu and U-B Eklind, *J. Nucl. Mater*. **297**, 231 (2001).
18. S. Sunder, G.D. Boyer and N.H. Miller, *J. Nucl. Mater*. **175**, 163 (1990).
19. F. King, M.J. Quinn and N.H. Miller, Swedish Nuclear Fuel and Waste Management Company Report, SKB TR-99-27 (1999).
20. J.C. Tait and L.H. Johnson, Proceedings of the Second International Conference on Radioactive Waste Management, Winnipeg, Canada, Sept. 7-11 (1986), Canadian Nuclear Society, Toronto, 611 (1986).